

## Neutron diffraction and the structure of amorphous $\text{Ni}_{0.95}\text{Tb}_{0.05}$

R. Fainchtein and J. S. Lannin

*Department of Physics, The Pennsylvania State University, University Park, Pennsylvania 16802*

D. L. Price

*Materials Science Division, Argonne National Laboratory, Argonne, Illinois 60439-4843*

(Received 30 June 1986)

Neutron diffraction measurements have been performed on amorphous  $\text{Ni}_{0.95}\text{Tb}_{0.05}$  and crystalline Ni. Thick dc-sputtered films of the amorphous alloy were prepared by high-rate triode magnetron sputtering into liquid-nitrogen-cooled substrates. The contributions of structural and thermal disorder to the first-neighbor radial distribution function were obtained using the crystalline Ni results along with corrections for finite  $Q_{\text{max}}$ . The results indicate a Ni-Ni first-neighbor structural disorder whose width,  $\sigma_1/\bar{r}_1 \approx 3\%$ , is substantially lower than values suggested for amorphous metals. Comparisons with theoretical models of the pair distribution function of  $a$ -Ni and  $a$ -Fe based on relaxed dense random-packed structures indicate good agreement with the results of Heimendahl. Density measurements have yielded the packing fraction for  $a$ - $\text{Ni}_{0.95}\text{Tb}_{0.05}$ . Extrapolation of this value has allowed an estimate of the packing fraction of pure  $a$ -Ni to be obtained. The results indicate a density greater than the maximum for a hard-sphere, dense random-packing model, but significantly below that of crystalline values found in some relaxed models.

### INTRODUCTION

Considerable interest in the structure of amorphous and liquid metals has evolved from theoretical models of dense-packed hard spheres.<sup>1-4</sup> Refinement of these models has involved use of softer repulsive potentials, as well as structural relaxation and Monte Carlo procedures.<sup>5-8</sup> Recent interest in the possibility of icosahedral order in amorphous metals and quasicrystalline materials has also revived interest in cluster models of intermediate-range order.<sup>9,10</sup> These various models and their detailed pair distribution functions and densities for amorphous transition metals have not been extensively compared, however, to experiment. Experimental studies of elemental amorphous transition metals have been constrained to *in situ* low-temperature electron diffraction studies due to thermal and thickness instabilities of these amorphous solids.<sup>11</sup> In addition, the density of very-thin-film amorphous transition metals is unknown. This implies that the radial distribution function and coordination numbers have not been obtained with accuracy. Similarly, a recent study of electrolytically prepared  $a$ -Fe at 300 K employed two-phase material with small amorphous particles of unknown density.<sup>12</sup>

Much of the experimental structural and physical property work in amorphous metals has thus involved alloy systems whose properties may differ considerably from that of pure elemental amorphous metals. Significant covalent interactions between transition metal (TM) and nonmetal ( $m$ ) atoms<sup>13</sup> or the presence of large concentrations of other metal atoms may result in substantial differences from single-atom models. In the present study a dilute alloy of Tb in  $a$ -Ni has been prepared in thick film form and studied by neutron diffraction. Although the presence of 5% Tb will influence the structure, its contribution to the Ni-Ni pair distribution function is

small for the first coordinate sphere. This allows an approximate comparison with theoretical calculations for  $a$ -Ni and  $a$ -Fe models. The stable, thick-film nature of the present system allows an accurate high wave-vector neutron diffraction determination of  $S(Q)$ , the total structure factor. In addition, the density of the system may be obtained and extrapolated to its approximate pure  $a$ -Ni value. This provides a means of obtaining the packing fraction which is found to have a value above that of the maximum dense random-packing (DRP) model, but below fcc, crystalline-like values, obtained in certain relaxed DRP models.

In addition to the alloy measurements, the radial distribution function of crystalline Ni has been obtained. This allows an estimate of the corresponding thermal broadening factor for the amorphous alloy Ni-Ni first-neighbor distribution. An approximate separation of this contribution from the total first-neighbor distance fluctuations provides a means of obtaining the static disorder parameter. Prior to this study, such measurements have not been made in amorphous metal systems. In the amorphous semiconductor  $a$ -Ge and  $a$ -Si, such studies<sup>14,15</sup> have been important in determining that the structural disorder in the first coordinate sphere is small. In contrast, in amorphous metals the absence of comparable covalent interactions is expected to result in a larger spread of first-neighbor distances that are of basic importance for an understanding of the structure and its resulting physical properties.

### EXPERIMENT AND DATA ANALYSIS

Both  $a$ - $\text{Ni}_{0.95}\text{Tb}_{0.05}$  and  $c$ -Ni thick films were prepared by triode magnetron sputtering at high rates. A sputtering pressure of 5 mTorr was employed with a cathode-

anode separation of 2.25 in. The system based pressure was  $3 \times 10^{-7}$  Torr and the sputtering rate was 850 Å/min. The amorphous sample was deposited on Al foil in thermal contact with a large plate cooled by liquid nitrogen. The *c*-Ni films were prepared on noncooled foils. Self-supported films of typical thickness 30 μm were analyzed by x-ray diffraction to determine their crystalline or amorphous state. These films were removed by simple peeling from the substrate. Neutron activation analysis confirmed that the film had the same 5 at. % Tb as the 2.25 in sputtering target, as well as indicated that little Ar (<1%) was incorporated in the films. Sample volume measurements were performed on a gas-phase autopycnometer (micrometric 1320) for the amorphous alloy. For improved accuracy a large, ~8 g, sample was employed. This volume was combined with microbalance mass measurements to obtain an alloy density of 8.43 g/cm<sup>3</sup>.

Neutron diffraction measurements were performed at 300 K at the Argonne National Laboratory Intense Pulsed Neutron Source on the SEPD (special environmental powder diffractometer) instrument. This instrument employs a broad, nonmonochromatic beam that is energy analyzed to obtain the wave vector  $Q$ . Time-of-flight measurements were performed on the samples, a reference V scatterer and an empty V container. The appropriately normalized detector intensities for angles of 15°, 30°, 60°, 90°, and 150° were corrected for absorption, container, and multiple scattering contributions.<sup>16</sup> The corrections were calculated at ten wavelengths and fit with polynomials. The packing density of the sample in the V container was employed as a variable so as to yield a structure factor,  $S(Q)$ , that oscillates about unity at high  $Q$  values. Values of  $Q_{\max} = 36$  and  $22 \text{ \AA}^{-1}$  were employed for *c*-Ni and for *a*-Ni<sub>0.95</sub>Tb<sub>0.05</sub>, respectively.

The normalized and background corrected intensities were employed to calculate an initial  $S(Q)$  which was utilized to obtain Placzek corrections point by point for each detector group. The Placzek correction utilized an effective temperature of 300 K. An analysis of the approximation form of the vibrational spectrum<sup>16</sup> of *a*-Ni indicates that this is a reasonable approximation. A weighted average of the different detector groups yields the final  $S(Q)$  which is Fourier transformed to obtain  $G(r)$  by the relation

$$G(r) = (2/\pi) \int_0^{Q_{\max}} Q [S(Q) - 1] \sin(Qr) M(Q) dQ, \quad (1)$$

where  $M(Q)$  is a damping or modification function. The Lorch<sup>17</sup> function  $M(Q) = \sin(\pi Q/Q_{\max})/\pi Q/Q_{\max}$ , as well as the undamped  $M(Q) = 1$  value were employed. The former, although reducing oscillatory noise in the reduced radial distribution function  $G(r)$  and the radial distribution function (RDF),  $J(r)$ , also reduces the resolution of the first- and second-neighbor peak in these functions.

The use of a finite  $Q_{\max}$  implies that spectral resolution is also reduced. Suzuki has studied this effect<sup>18</sup> for a single Gaussian shaped peak and obtained curves that may be utilized to approximately correct for finite  $Q_{\max}$ . Using his universal curves in terms of  $Q_{\max}^* \equiv Q_{\max} \bar{r}_1$ , where  $\bar{r}_1$  is the mean first-neighbor distance, we have self-consistently estimated the correction factor for *a*-

Ni<sub>0.95</sub>Tb<sub>0.05</sub> and *c*-Ni. The correction factor for the width of the first-neighbor RDF peak for *c*-Ni for  $M(Q) = 1$  spectra is 0.98, while for *a*-Ni<sub>0.95</sub>Tb<sub>0.05</sub> the factor is 0.95. While these approximate correction factors are relatively small here for  $Q_{\max} \geq 20 \text{ \AA}^{-1}$ , Suzuki's calculations clearly indicate that such corrections are nonlinear in  $Q_{\max}$  and thus may be significant at lower  $Q_{\max}$  values employed in a number of previous studies.<sup>19</sup> For values of  $Q < Q_{\min} = 0.7 \text{ \AA}^{-1}$ ,  $S(Q)$  was extrapolated to  $Q = 0$  using a quadratic dependence on  $Q$ .

## RESULTS AND DISCUSSION

Shown in Fig. 1 is the radial distribution function obtained in Eq. (1) for *c*-Ni using a Lorch damping and the relation

$$J(r) = rG(r) + 4\pi r^2 \rho_0. \quad (2)$$

The density,  $\rho_0$ , employed in Eq. (2) was that of bulk *c*-Ni and is an upper limit to that of the thick-film material. The form of  $J(r)$  in Fig. 1 is quite similar to the expected form for fcc Ni. The peaks in  $J(r)$  are finite in width due to contributions from thermal disorder and the effects of the damping function, finite  $Q_{\max}$  and instrumental resolution. The first and second coordination regions are shown in Fig. 2 for both  $M(Q) = 1$  and for the Lorch function. While the damping function reduces termination oscillations, it clearly increases the width of the first two peaks in the RDF relative to undamped termination. The width of the latter yields an improved estimate of the thermal broadening of *c*-Ni. The further correction for finite  $Q_{\max}$ , discussed above, narrows this width by an additional 2%. The resulting thermal width of *c*-Ni for the first RDF peak is  $(\sigma_1)_{\text{th}} = 0.077 \text{ \AA}$ , corresponding to  $(\sigma_1)_{\text{th}}/\bar{r}_1 = 3.1\%$ . This value is 14% smaller than that predicted by a simple Debye theory.<sup>20</sup> However, when coupling between first neighbors and the atom at the origin is incorporated into the theory,<sup>21</sup> the experimental result is only 5% smaller than the predicted value. Preliminary analysis of the data<sup>22</sup> led to slightly higher values of  $\sigma_1$  for *c*-Ni and *a*-Ni<sub>0.95</sub>Tb<sub>0.05</sub>.

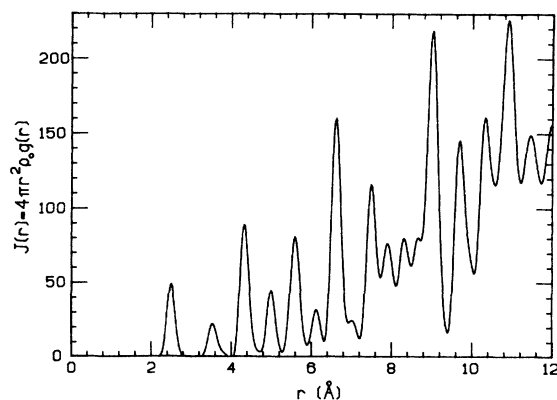


FIG. 1. Radial distribution function of crystalline Ni at 300 K with Lorch termination for  $Q_{\max} = 36 \text{ \AA}^{-1}$ .

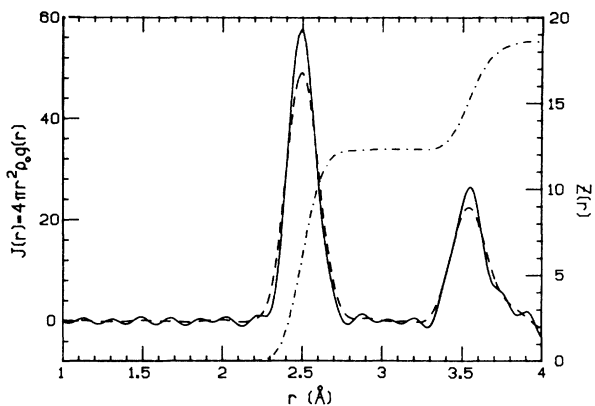


FIG. 2. Radial distribution function  $J(r)$  of crystalline Ni at 300 K with (dashed line) and without (solid line) Lorch termination for  $Q_{\max} = 36 \text{ \AA}^{-1}$ . Coordination number  $Z(r)$  of the same sample as a function of radial distance from an atomic site (dotted-dashed line).

The coordination number,  $Z(r) = \int_0^r J(r') dr'$ , is shown in Fig. 2 for Lorch damping. Similar results are obtained for  $M(Q) = 1$ . The values of 12.3 and 18.5 obtained for the first and second coordination numbers are near to the fcc values of 12 and 18, respectively. The 2–4% larger values may in part be a consequence of the somewhat lower film density than that of bulk Ni employed in determining the RDF.

The form of  $S_0(Q)$  for  $a\text{-Ni}_{0.95}\text{Tb}_{0.05}$  is shown in Fig. 3 for  $Q_{\max} = 22 \text{ \AA}^{-1}$ . The resulting  $G(r)$  using Lorch damping and  $M(Q) = 1$  are shown in Fig. 4. The slope of the low  $r$  region yields a density,  $\rho_0 = -4\pi G(r)/r$  which agrees within a few percent with the measured value of  $8.43 \text{ g/cm}^3$ . For  $c\text{-Ni}$ , the slope of  $G(r)$  at low  $r$  is also found to be within its bulk range. The  $J(r)$  obtained with the bulk value of the density is shown in Fig. 5 for  $r < 12 \text{ \AA}$ . Clearly defined radial correlations are present here and in  $G(r)$  up to large values of  $r$  in these alloys. Such

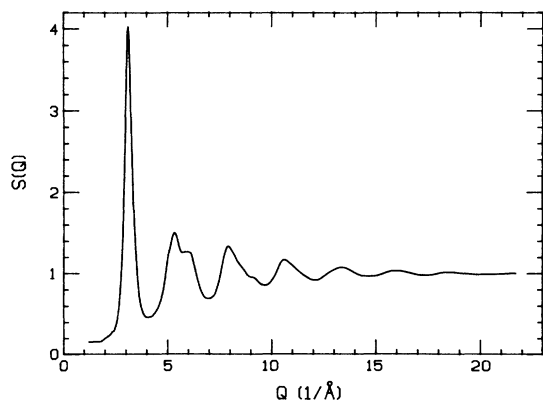


FIG. 3. Total structure factor of amorphous  $\text{Ni}_{0.95}\text{Tb}_{0.05}$  at 300 K.

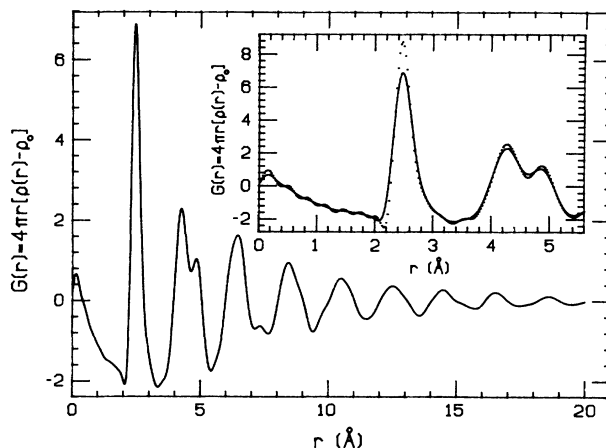


FIG. 4. Reduced radial distribution function  $G(r)$  of amorphous  $\text{Ni}_{0.95}\text{Tb}_{0.05}$  with Lorch termination for  $Q_{\max} = 22 \text{ \AA}^{-1}$ . The inset shows the first two peaks with (solid line) and without (dotted line) Lorch termination.

oscillations are similar to those observed in amorphous transition metal-metalloid alloys.<sup>19,23</sup> A higher resolution RDF is shown for  $r < 6 \text{ \AA}$  in Fig. 6 for the case of  $M(Q) = 1$ . For comparison, the Lorch damping result is also shown. As in  $c\text{-Ni}$  the latter reduces the resolution of the lower  $r$  peaks in  $J(r)$ . Certain weak shoulder features seen at  $r \approx 3.6 \text{ \AA}$  and  $5.6 \text{ \AA}$  appear to be present for both  $M(Q)$  choices, suggesting that they are not artifacts of the data analysis.

As may be clearly seen in Fig. 6, the first peak in  $J(r)$  is asymmetric in form. This result is similar to that obtained for both DRP structures, as well as relaxed DRP models, and is a consequence of repulsive interactions at small  $r$ . The first peak of the RDF yields the approximate mean position of the nearest neighbors; this occurs at  $2.48 \text{ \AA}$  which is 0.5% below the  $c\text{-Ni}$  value. To obtain an estimate of the structural disorder in the  $a\text{-Ni}_{0.95}\text{Tb}_{0.05}$  amorphous film, the width of the first peak to lower  $r$

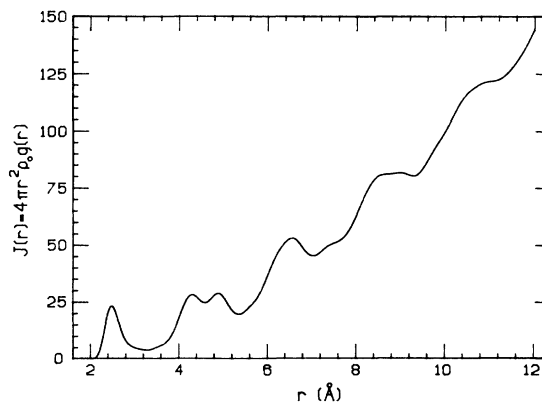


FIG. 5. Radial distribution function  $J(r)$  of amorphous  $\text{Ni}_{0.95}\text{Tb}_{0.05}$  at 300 K with Lorch termination.

values has been employed. A Gaussian fit to this portion of the peak was employed to obtain the width for the  $M(Q)=1$  case. This width was further self-consistently corrected as in *c*-Ni for finite  $Q_{\max}$ . This yields a correction of 5% to the width shown in Fig. 6. The total effective Gaussian width of the lower portion of the first RDF peak is found to be  $(\sigma_1)_{\text{total}}/\bar{r}_1=4.2\%$ .

The width of the lower half of the first RDF peak corrected for finite  $Q_{\max}$  corresponds to a total thermal plus structural disorder normalized width  $(\sigma_1/\bar{r}_1)\simeq 4\%$ . The independence of these contributions and their approximate Gaussian forms suggests that  $(\sigma_1)_m^2=(\sigma_1)_{\text{th}}^2+(\sigma_1)_d^2$ , where  $(\sigma_1)_d$  is the static structural disorder contribution and  $(\sigma_1)_m$  is the measured  $e^{-1}$  width. The thermal contribution may be estimated to be that of *c*-Ni as a first approximation. This yields a relative disorder  $(\sigma_1)_d/\bar{r}_1\simeq 3\%$  for the lower  $r$  portion of the first coordination sphere. As the *a*-Ni<sub>0.95</sub>Tb<sub>0.05</sub> peak is asymmetric the use of Gaussian additivity of disorder contributions is only an approximation. An independent estimate of the structural disorder may be obtained by deconvolving the experimental  $J(r)$  using the thermal disorder of *c*-Ni. This procedure yields  $(\sigma_1)_d/\bar{r}_1\simeq 3\%$ , indicating that the assumption  $(\sigma_1)_m^2=(\sigma_1)_{\text{th}}^2+(\sigma_1)_d^2$  is a good approximation. This value is comparable to the estimated thermal disorder and contrasts with amorphous semiconductors where  $(\sigma_1)_{\text{th}}$  is substantially larger than  $(\sigma_1)_d$ .<sup>14,15</sup>

The value of  $\sim 3\%$  for the structural disorder for the first coordination sphere width is considerably lower than the 5–6% value estimated for *a*-TM-*m* alloys.<sup>19</sup> This is, in part, a consequence of the significant thermal disorder contribution, as well as the need for significantly larger corrections for lower  $Q_{\max}$  values than those employed here. An analysis, for example, of the first  $J(r)$  peak<sup>23</sup> for Ni-Ni correlations in *a*-Ni<sub>0.81</sub>B<sub>0.19</sub>, indicates after correcting for thermal broadening and finite  $Q_{\max}$ , a similar value for the static disorder. The lower experimental  $Q_{\max}$  of 13 Å<sup>-1</sup> in this case yields an estimated termina-

tion correction factor of 0.7.

The integral of  $J(r)$  of Fig. 6 yields for a binary alloy a neutron weighted coordination number,  $Z'(r)$ :<sup>24</sup>

$$Z'(r)=\int_0^r\left[\sum_{i,j=1}^2w_{ij}rG_{ij}(r)+4\pi r^2\rho_0\right]dr. \quad (3)$$

The neutron weighting factors  $w_{ij}=x_i x_j b_i b_j / \langle b \rangle^2$ , where  $x_i$  and  $b_i$  are the concentration and coherent scattering lengths for species  $i$ . For *a*-Ni<sub>0.95</sub>Tb<sub>0.05</sub> these have the values of  $w_{\text{Ni-Ni}}=0.927$  and  $w_{\text{Ni-Tb}}=0.036$  and  $b_{\text{Ni}}=10.3$  fm,  $b_{\text{Tb}}=7.6$  fm. The observed  $Z'(r)$  is shown in Fig. 6. Theoretical calculations of  $Z'(r)$  for the related *a*-Co<sub>1-x</sub>Gd<sub>x</sub> system<sup>25</sup> indicate, for low Tb concentration, that at low  $r$  ( $< 1.15\bar{r}_1$ ) it is dominated by Ni-Ni correlations. This is a physical consequence of the significantly larger Tb size and constraints on atom approach distances for modified hard-sphere constraints. For larger values of  $r$ , contributions from Tb atoms influence  $J(r)$  and  $G(r)$  in selected regions. This is particularly the case where  $G_{\text{Ni-Ni}}(r)$  is small. Figure 6 indicates for  $r=3.3$  Å corresponding to the minimum in the RDF beyond the first peak, an effective coordination number  $Z'\simeq 11.9$ . Although this number is a weighted value, it is estimated to be rather close to the value of the total  $Z$  obtained if Ni and Tb were to have similar scattering strengths. This is a consequence of the dominance of the Ni-Ni term in Eq. (3).

It is also possible, in an approximate sense, to extrapolate the results for the 95% Ni alloy to that of a hypothetical pure *a*-Ni system. Calculations of Cargill<sup>25</sup> of *a*-Co<sub>1-x</sub>Gd<sub>x</sub>, using a relaxed DRP model, support an approximate 5% increase in density of the pure *a*-Co over the 95% alloy. Comparisons of his  $J(r)$  values indicate that the effective coordination number of the 95% alloy is approximately 5% below that of pure *a*-Co. This suggests that the alloy  $Z'$  number is comparable to or perhaps of order 5% less than the coordination number expected for a hypothetical pure *a*-Ni system. For pure *a*-Co the theoretical results indicate a coordination of  $11.85\pm 0.5$ . Although  $Z'(r)$  for *a*-Ni<sub>0.95</sub>Tb<sub>0.05</sub> has a contribution from Ni-Tb correlations, it is useful to compare its form to that of *c*-Ni in Fig. 2 in a semiquantitative manner. The differences in these  $J(r)$  with increasing  $r$  indicate the more gradual rise to a crystallike coordination in the amorphous state. This is a consequence of structural disorder and a locally lower density in the metastable amorphous system.

A comparison of the experimental pair distribution function  $g(r)=J(r)/4\pi r^2\rho_0$  for *a*-Ni<sub>0.95</sub>Tb<sub>0.05</sub> and that of models<sup>5,6</sup> of pure *a*-Ni and *a*-Fe is shown in Figs. 7 and 8. The theoretical results have been broadened by the 3.1% thermal disorder obtained for the first peak of pure *c*-Ni (Ref. 26) and the *a*-Ni<sub>0.95</sub>Tb<sub>0.05</sub> correction factor for finite  $Q_{\max}$ . The experimental and theoretical spectra have been normalized to the first peak in  $g(r)$ . The theoretical results<sup>6</sup> of Maeda *et al.*, based on a Monte Carlo modeling of *a*-Fe which employed a Johnson potential, do not agree well with the present alloy  $g(r)$ . Of particular importance is the position of the second peak in the experiment at  $r_2=1.72\bar{r}_1$ , whereas this theory has  $r_2\simeq 1.66\bar{r}_1$ . Similar

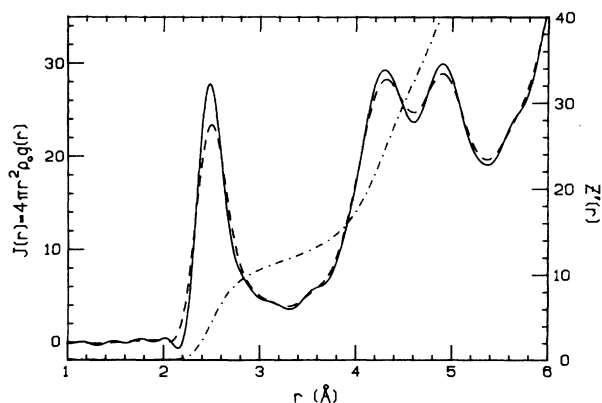


FIG. 6. Radial distribution function  $J(r)$  of amorphous Ni<sub>0.95</sub>Tb<sub>0.05</sub> at 300 K with (dashed line) and without (solid line), Lorch termination. Neutron weighted coordination number  $Z'(r)$  of the same sample as a function of radial distance from an atomic site (dotted-dashed line).

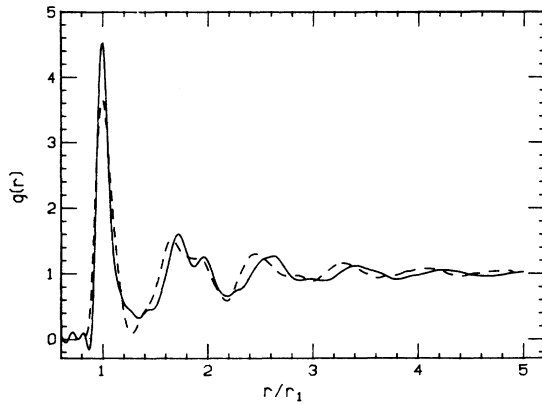


FIG. 7. Pair distribution function  $g(r)$  of amorphous  $\text{Ni}_{0.95}\text{Tb}_{0.05}$  at 300 K with  $M(Q)=1$  in Eq. (1) (solid line). Maeda and Takeuchi model (Ref. 7) of  $g(r)$  broadened with  $(\sigma_1)_{\text{th}}/\bar{r}_1=3.1\%$  (dashed line). The curves have been normalized to the position of the first peak.

results are obtained for the results of Doyama and Yamamoto<sup>7</sup> whose relaxed DRP has  $r_2 \approx 1.66\bar{r}_1$ . At larger values of  $r$  the experimental peaks in Fig. 7 are also seen to occur at larger values than that of theory. While the effects of Tb might be expected to yield this effect, an analysis of the relaxed DRP model<sup>25</sup> of  $a\text{-Co}_{1-x}\text{Gd}_x$  system for  $x=0.05$  indicates that the rare-earth contributions are not sufficiently large to significantly change the positions of the major peaks in  $g(r)$  or  $G(r)$  as a first approximation.

The comparison with the relaxed DRP model of  $a\text{-Ni}$  of Heimendahl<sup>5</sup> shown in Fig. 8 yields better agreement with experiment. This is also shown in the inset of Fig. 8, where a more dense, thermal broadened theoretical histogram was employed for the nearest-neighbor distribution. While the theoretical  $g(r)$  is slightly wider than the exper-

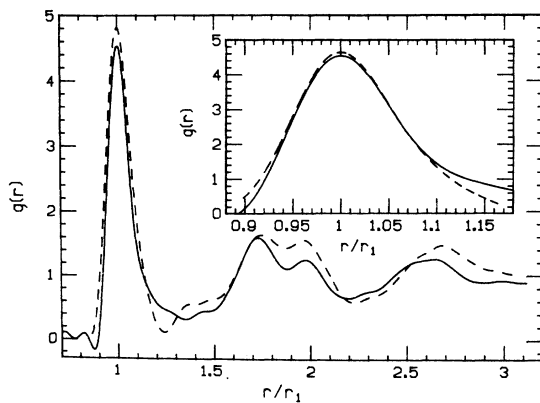


FIG. 8. Pair distribution function  $g(r)$  of amorphous  $\text{Ni}_{0.95}\text{Tb}_{0.05}$  at 300 K with  $M(Q)=1$  in Eq. (1) (solid line). Heimendahl model (Ref. 5) of  $g(r)$  broadened with  $(\sigma_1)_{\text{th}}/\bar{r}_1=3.1\%$  (dashed line). The curves have been normalized to the position of the first peak. The inset shows the first peak obtained from a finer histogram of the model.

iment, the results indicate considerable similarity between spectra. Beyond  $r \approx 1.17\bar{r}_1$  the experimental  $g(r)$  is larger than the theoretical result. In this region  $g(r)$  is small for Ni-Ni correlations. As such, contributions from Ni-Tb and Tb-Ni terms in  $g(r)$  are the likely origin of the differences. The trend observed in the region between  $r=1.2-1.67\bar{r}_1$  is similar to that obtained from a comparison of  $g(r)$  for  $a\text{-Co}$  and an 8% Gd alloy. Differences between the theoretical results of Heimendahl and the alloy  $g(r)$  for the peak near  $r=2\bar{r}_1$  do not appear, however to arise from Tb contributions as here the  $G_{ij}(r)$  are all of the same sign and do not interfere. Similarly, the somewhat larger value of the theoretical maxima and minima for  $r > 2.2\bar{r}_1$  do not appear to be due to the Tb contribution. Further calculations for the  $a\text{-Ni}_{0.95}\text{Tb}_{0.05}$  system using a relaxed DRP model would be useful to confirm this, as well as determine the conditions for improved theoretical spectra. Clearly further measurements of the Tb contribution to the  $G(r)$  and  $g(r)$  are also required to more accurately quantify the role of Tb.

The bulk density of  $a\text{-Ni}_{0.95}\text{Tb}_{0.05}$  allows a determination of the equivalent hard-sphere packing fraction. From the relation<sup>25</sup>  $F_p = (4\pi/3)\rho_a \langle R^3 \rangle$ , where  $\langle R^3 \rangle = 0.95r_{\text{Ni}}^3 + 0.05r_{\text{Tb}}^3$ , and estimated values of  $r_{\text{Ni}}=1.245 \text{ \AA}$  and  $r_{\text{Tb}}=1.72 \text{ \AA}$ ,<sup>27</sup> the  $F_p=0.70$  is obtained. From this result it is also possible to estimate the approximate value for pure  $a\text{-Ni}$ . Model relaxed DRP calculations for the  $a\text{-Co}_{1-x}\text{Gd}_x$  system yield an approximate 5.5% greater density for  $x=0$  relative to  $x=0.95$ . This system is expected to have rather similar ratios of atomic sizes and interatomic interactions as that of  $a\text{-Ni}_{1-x}\text{Tb}_x$  so that the theoretical results serve as a first approximation here. Assuming a similar density change for dilute Tb in  $a\text{-Ni}$  and a Ni radius of one half  $\bar{r}_1$  yields an estimated packing fraction of 0.68 for pure  $a\text{-Ni}$ . This value is in good agreement with the value of 0.68 obtained in the relaxed DRP calculation<sup>25</sup> for pure  $a\text{-Co}$ . It is useful to note that this exceeds by 6.6% the maximum value of the  $F_p=0.637$  obtained from a hard-sphere model.<sup>2</sup> In addition, this value is near the lower estimate for pure  $a\text{-Fe}$  obtained by the Monte Carlo procedure of Maeda and Takenchi,<sup>6</sup> but 9% below that of the crystallike upper limit. It is possible, however, that the present density is, in part, a consequence of deposition conditions and that larger values of the density and packing fraction are possible in annealed  $a\text{-Ni}_{0.95}\text{Tb}_{0.05}$  alloys.

In summary, the neutron diffraction spectra of  $a\text{-Ni}_{0.95}\text{Tb}_{0.05}$  for  $Q_{\text{max}}=22 \text{ \AA}^{-1}$  have been employed to obtain detailed information about the Ni first-neighbor local order. As this local order for  $r < 1.17\bar{r}_1$  is dominated by Ni-Ni correlations, comparison with theoretical studies of pure amorphous transition metals may be employed for comparison. The separation of the radial disorder into thermal and static disorder contributions is found to yield a 3% value for the latter. This value is considerably lower than previous estimates of the spread of the first-neighbor distribution obtained for other experimental studies due to both thermal and finite  $Q_{\text{max}}$  effects. The form of the thermally broadened first-neighbor peak is found to be similar to that of the relaxed DRP model of Heimendahl. The additional asymmetry of the experi-

ment versus theory may well be a consequence of Ni-Tb correlations that have not been addressed here. At larger  $r$  values the Heimendahl model also yields better agreement for the second-neighbor peak than that of models employed for  $a$ -Fe. Although Tb-Ni correlations may modify somewhat the  $G(r)$  and  $J(r)$  results relative to pure  $a$ -Ni, comparison with theoretical results for the related  $a$ -Co<sub>1-x</sub>Gd<sub>x</sub> system suggest that these corrections are not large. Thus the peaks in these functions are not predicted to substantially change as Tb is reduced below 5%. Further measurements would be useful, however, to more precisely quantify the relation to models of pure  $a$ -Ni.

In contrast to previous electron diffraction studies of  $a$ -Ni, the present thick-film material has allowed more accurate density measurements to be obtained. The results indicate a density that is greater than that of hard spheres,

but substantially below that of fcc  $c$ -Ni. This does not imply, however, that greater densities cannot be achieved with annealing, for example. Further studies are in progress in this regard.

#### ACKNOWLEDGMENTS

We wish to thank Dr. L. Pilione for determining the film composition and Ar content, Dr. S. Susman for assistance with the pycnometer measurements, Dr. S. Cargill for detailed information on  $a$ -Co<sub>1-x</sub>Gd<sub>x</sub> alloy calculations, and Dr. J. Carpenter for useful discussions. This work was supported at The Pennsylvania State University under U.S. Department of Energy (DOE) Grant No. DE-FG02-84ER45095. One of us (D.L.P.) acknowledges support under DOE Grant No. W-31-109-Eng-38.

- 
- <sup>1</sup>J. D. Bernal, Proc. R. Soc. London, Ser. A **284**, 299 (1964); G. Mason, Faraday Soc. Discuss. **43**, 75 (1967).
- <sup>2</sup>J. L. Finney, in *Amorphous Metallic Alloys*, edited by F. E. Luborsky (Butterworth, London, 1983), p. 42, and references therein.
- <sup>3</sup>C. H. Bennett, J. Appl. Phys. **43**, 2727 (1972).
- <sup>4</sup>T. Ichikawa, Phys. Status Solidi A **29**, 293 (1975).
- <sup>5</sup>L. v. Heimendahl, J. Phys. F **5**, L141 (1975).
- <sup>6</sup>R. Yamamoto, H. Matsuoka, and M. Doyama, J. Phys. F **7**, L43 (1977).
- <sup>7</sup>K. Maeda and S. Takeuchi, J. Phys. F **8**, L283 (1978).
- <sup>8</sup>M. Doyama and R. Yamamoto, in *Amorphous Materials: Modeling of Structure and Properties*, edited by V. Vitek (American Institute of Mining, Metallurgy and Petroleum Engineering, New York, 1983), p. 243.
- <sup>9</sup>J. A. Barker, J. Phys. (Paris) Colloq. **38**, C-2, 37 (1977).
- <sup>10</sup>S. Sachdev and D. R. Nelson, Phys. Rev. Lett. **53**, 1947 (1984).
- <sup>11</sup>T. Ichikawa, Phys. Status Solidi A **19**, 707 (1973).
- <sup>12</sup>J. P. Lauriat, J. Non-Cryst. Solids **55**, 77 (1983).
- <sup>13</sup>N. Lustig, J. S. Lannin, D. L. Price, and R. Hasegawa, J. Non-Cryst. Solids, **75**, 277 (1985).
- <sup>14</sup>R. Temkin, G. A. N. Connell, and W. Paul, Adv. Phys. **22**, 581 (1973).
- <sup>15</sup>S. C. Moss and J. F. Graczyk, Phys. Rev. Lett. **23**, 1167 (1969).
- <sup>16</sup>R. Yamamoto, K. Haga, T. Mihara, and M. Doyama, J. Phys. F **10**, 1389 (1980).
- <sup>17</sup>E. A. Lorch, J. Phys. C **2**, 229 (1969).
- <sup>18</sup>K. Suzuki, in *Amorphous Metallic Alloys*, Ref. 2, p. 78.
- <sup>19</sup>P. H. Gaskell, in *Glassy Metals II*, edited by H. Beck and H.-J. Güntherodt (Springer-Verlag, Berlin, 1983), p. 16, and references therein.
- <sup>20</sup>B. T. M. Willis and A. W. Pryor, *Thermal Vibrations in Crystallography* (Cambridge University Press, London, 1975), p. 136.
- <sup>21</sup>N. J. Shevchik, Ph.D. thesis, Harvard University, U.S. Office of Naval Research Technical Reports Nos. HP-29 and ARPA-44, 1972 (unpublished), p. III-1.
- <sup>22</sup>R. Fainchtein, J. S. Lannin, and D. L. Price, in Proceedings of the 6th International Conference on Liquid and Amorphous Metals (unpublished).
- <sup>23</sup>P. Lamparter, W. Sperl, and S. Steeb, Z. Naturforsch. Teil A **37**, 1223 (1982).
- <sup>24</sup>Y. Waseda, *The Structure of Non-Crystalline Materials* (McGraw-Hill, New York, 1980).
- <sup>25</sup>G. S. Cargill, in *Amorphous Materials: Modeling of Structure and Properties*, Ref. 8, p. 15.
- <sup>26</sup>The broadening parameter for the second RDF peak of  $c$ -Ni is  $\sim 1.4$  times greater than for the first peak. The contribution of the estimated thermal broadening to the theoretical results in Fig. 7 are thus a lower limit for the second and higher peaks in  $g(r)$ .
- <sup>27</sup>J. J. Rhyne, *Magnetism and Magnetic Materials*, Proceedings of the 19th Annual Conference on Magnetism and Magnetic Materials, AIP Conf. Proc. No. 18, edited by C. D. Graham and J. J. Rhyne (AIP, New York, 1974), p. 563.